

# The spall strength limit of matter at ultrahigh strain rates induced by laser shock waves

V.E. FORTOV,<sup>1</sup> D. BATANI,<sup>2</sup> A.V. KILPIO,<sup>3</sup> I.K. KRASYUK,<sup>3</sup> I.V. LOMONOSOV,<sup>4</sup> P.P. PASHININ,<sup>3</sup>  
E.V. SHASHKOV,<sup>3</sup> A.YU. SEMENOV,<sup>3</sup> AND V.I. VOVCHENKO<sup>3</sup>

<sup>1</sup>Institute for High Energy Density RAS, 13/19 Izhorskaya Street, Moscow 127412, Russia

<sup>2</sup>Dipartimento di Fisica “G. Occhialini” and INFN, Università degli Studi di Milano–Bicocca,  
Piazza della Scienza 3, 20126 Milano, Italy

<sup>3</sup>General Physics Institute of the Russian Academy of Sciences (RAS), 38 Vavilov Street, Moscow 119991, Russia

<sup>4</sup>Institute of Chemical Physics Problems at Chernogolovka RAS, Chernogolovka 142432, Russia

(RECEIVED 4 January 2002; ACCEPTED 5 February 2002)

## Abstract

New results concerning the process of dynamic fracture of materials (spallation) by laser-induced shock waves are presented. The Nd-glass laser installations SIRIUS and KAMERTON were used for generation of shock waves with pressure up to 1 Mbar in plane Al alloy targets. The wavelengths of laser radiation were 1.06 and 0.53  $\mu\text{m}$ , the target thickness was changed from 180 to 460  $\mu\text{m}$ , and the laser radiation was focused in a spot with a 1-mm diameter on the surface of AMg6M aluminum alloy targets. Experimental results were compared to predictions of a numerical code which employed a real semiempirical wide-range equation of state. Strain rates in experiments were changed from  $10^6$  to  $5 \times 10^7 \text{ s}^{-1}$ . Two regimes of spallation were evidenced: the already known dynamic regime and a new quasi-stationary regime. An ultimate dynamic strength of 80 kbar was measured. Finally, experiments on targets with artificial spall layers were performed showing material hardening due to shock-wave compression.

**Keywords:** Laser shock wave; Spallation; Strength limit

## 1. INTRODUCTION

Lasers provide an unique possibility to study the characteristics of matter in extreme states in the laboratory. This article presents the results of investigation of the mechanical properties of the AMg6M aluminum alloy under strain rates up to  $10^7 \text{ s}^{-1}$ . The alloy AMg6M is made of Al with 0.3–0.6% Mn and 5.5–6.5% Mg (the last letter M stands for “soft”).

We determined the dynamic strength of matter by studying the spallation phenomena (Zel’dovich & Raizer, 1967; Bushman *et al.*, 1993) as shown in Figure 1. The experimental results included the upper limit of dynamic strength of the material under investigation. Two different regimes of dynamic fracture were evidenced.

Under the action of a short, intensive laser pulse focused on the target surface, a strong shock is formed and propagates into the target (see Fig. 2). The shock wave reflects

from the rear surface of the target and transforms into a negative pressure pulse travelling backwards in the material. This pulse quickly increases up to a maximum value and then slowly drops down. A tensile stress (negative pressure) is then created which can exceed the dynamic strength of the material at some distance from the rear surface of the target (between  $h_1$  and  $h_2$ , see Fig. 2). The thickness of the fracture (spallation) zone is zone  $\delta h = h_1 - h_2$  (see Fig. 2). Here the spallation process can occur, that is, the fracture of the material and the separation of a rear layer of the target. To determine the value of the spall strength, we experimentally measured (1) the spall layer thickness  $h_1$  (or  $h_2$ ), and (2) the time  $t_{arr}$  at which the spall layer arrives at the electrocontact sensor at a fixed distance  $L$  (see Fig. 3). These experimental results were there compared to, and analyzed with, the help of numerical calculations of the pressure evolution in the spall plane.

The targets with an artificial spall layer consists of two layers of Al alloy glued together. The thickness of the glue is a few microns, while the thickness of the artificial spall layer is 8–50  $\mu\text{m}$  and the thickness of the main target is 210–400  $\mu\text{m}$ .

Address correspondence and reprint requests to: Igor Krasyuk, General Physics Institute of the Russian Academy of Sciences, 38 Vavilov Street, Moscow 119991, Russia. E-mail: krasyuk@kapella.gpi.ru

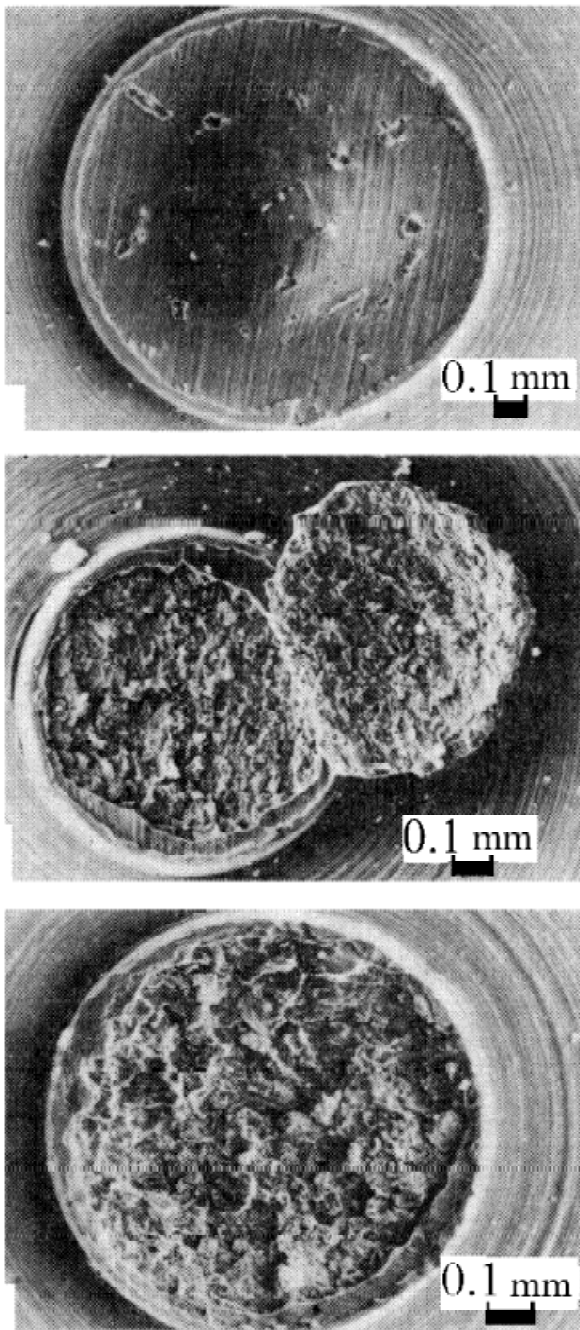


**Fig. 1.** Results of the laser-induced spallation process. When the ablation pressure on the front surface of the target increases, it is possible to observe (top to bottom): the appearance of spallation in the center of the target (154 kbar), its development (187 kbar), and its completion with the full separation of a spall layer from the target (247 kbar). Here 154, 187, and 247 kbar are the values of ablation pressures on the front sides of the targets. In this experiment, the maximum value of ablation pressure was 686 kbar. These should not be confused with the value of 80 kbar, that is, the negative pressure (spall strength) in the plane of spallation.

## 2. EXPERIMENTS

The experiments were carried out with the Nd-glass laser installations KAMERTON and SIRIUS (General Physics

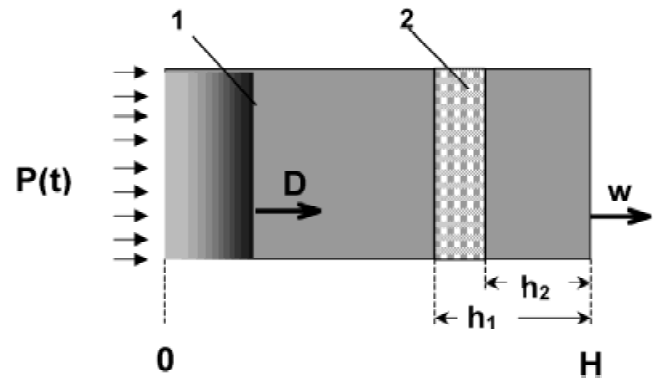


**Fig. 2.** The scheme of shock wave interaction with the target. 1: shock-wave front, 2: fracture zone,  $D$ : velocity of the shock-wave front, and  $w$ : velocity of rear side of target.

Institute of the Russian Academy of Sciences). The parameters of KAMERTON are the following: radiation wavelength  $0.53 \mu\text{m}$ , maximum energy in the pulse up to 100 J, duration of the laser pulse 2.5 ns. The parameters of SIRIUS are: wavelength  $1.06 \mu\text{m}$ , maximum energy up to 60 J, duration of laser pulse 5–80 ns, and the laser pulse may have Gaussian, square, or triangular shapes. For reducing boundary effects, the targets had a salient on their rear side, with a thickness approximately equal to the expected maximal value of the spall layer ( $100 \mu\text{m}$ ). Targets had a thickness in the range 180 to  $460 \mu\text{m}$ . The laser focal spot diameter was 1 mm. The thickness of the fracture zone  $\delta h$  is equal to 2–50  $\mu\text{m}$ .

The scheme of the experiments is shown in Figure 3: the time at which the spall layer reaches the electrocontact sensor aligned at distance  $L$  is measured with a Tektronix TDS-744A oscilloscope. The distance  $L$  in the experiment was changed from 110 to 880  $\mu\text{m}$ .

## 3. NUMERICAL MODELING

Target design was optimized by using a two-dimensional numerical code which takes into account elastic and plastic processes (Ivanov & Petrov, 1992). A one-dimensional hydrodynamic numerical code (Semenov, 1997) with a wide-range real equation of state (EOS) for aluminum (Bushman *et al.*, 1993) was used for modeling the shock-wave inter-

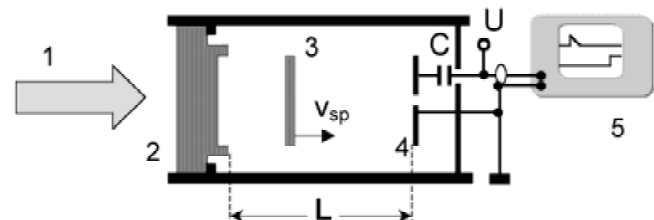


**Fig. 3.** The scheme of the experiment. 1: laser beam, 2: target, 3: spall layer, 4: electrocontact sensor, 5: oscilloscope.  $v_{sp}$  is the velocity of the spall layer. 5: Here  $U = 9 \text{ V}$  and  $C = 0.01 \mu\text{F}$ .

action with targets (Batani *et al.*, 1999a,b). In the calculations, we assumed that the temporal shape of the pressure pulse is the same of the laser pulse. The ablation pressure  $P$  was estimated using well-known scaling laws:

$$P \text{ (kbar)} = 28 (I/10^{11})^{1.5} \quad \text{for } 4 \times 10^{10} < I < 3 \times 10^{11}$$

following Vovchenko *et al.* (1994) and

$$P \text{ (Mbar)} = 14 (I/10^{14})^{7/2} \lambda^{-2/9} \\ \text{for } 3 \times 10^{11} < I < 4.5 \times 10^{12}$$

$$P \text{ (Mbar)} = 12 (I/10^{14})^{2/3} \lambda^{2/3} Z^{3/16} \\ \text{for } 4.5 \times 10^{12} < I < 2 \times 10^{15} \text{ and } Z = 4 - 14$$

(Dahmani, 1993). Here  $I$  is intensity of laser radiation on the surface of target measured in watts per centimeter squared,  $\lambda$  is the laser wavelength in microns, and  $Z$  is the atomic number of the target material.

The numerical modeling allows to calculate the nonstationary distribution of the thermodynamic parameters in the target material under the action of a pressure pulse. Calculation of the pressure evolution in the various cross sections of the target shows that near the rear target surface, the negative pressure pulse has a sharp front and long tail, while inside the target, the negative pressure pulse becomes more symmetric.

#### 4. MAIN EQUATION FOR $t_{sp}$

The method for determining the time of spallation  $t_{sp}$  is based on comparing the experimental data and the numerical modeling. The thickness of the spall layer,  $h_{sp}$  ( $= h_1$  or  $h_2$ ), and the arrival time of the spall layer at the electrocontact sensor  $t_{arr}$  were experimentally measured. The profiles of pressure  $P(t)$  in the spall planes  $h_{sp}$ , and the value of the strain rate

$$\dot{V} = \frac{1}{\rho_0} \frac{d\rho}{dt}$$

were obtained from the numerical modeling, Here  $\rho_0$  is the initial density of matter. To determine  $t_{sp}$  we solved nonlinear equation

$$t_{sp} + L/v_{sp} = t_{arr} \quad (1)$$

where

$$v_{sp} = \left( \int_0^{t_{sp}} P(t) dt \right) / m_{sp},$$

and  $m_{sp} = \rho_0 h_{sp}$  is the mass of spall layer per unit of target surface. Here  $t = 0$  corresponds to the arrival of the laser pulse on the target front side.

After determining  $t_{sp}$ , we calculated the spall strength  $\sigma^*$  as

$$\sigma^* = |P(t_{sp})|$$

in the plane  $h_{sp}$ .

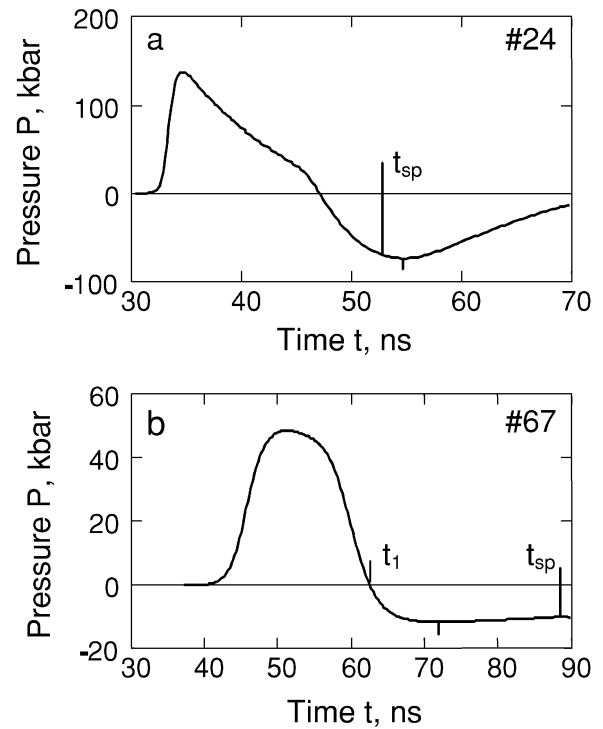


**Fig. 4.** The pressure profiles ( $P = P(t)$ ) in the fracture plane in case of dynamic (a) and quasi-stationary (b) regimes of spallation according to the results of simulations. Also shown the time  $t_{sp}$ , found by means of Eq. (1).

It was proposed that the process of material fracture occurs instantaneously when the negative pressure in a definite cross section of target is more than the material strength. In reality the process of target fracture in a spall plane has a finite time duration. The method used permits us to measure only an average value of this time duration when a narrow spall disc separates from the target. The improvement of the method must include direct measurement of the velocity of the spall layer.

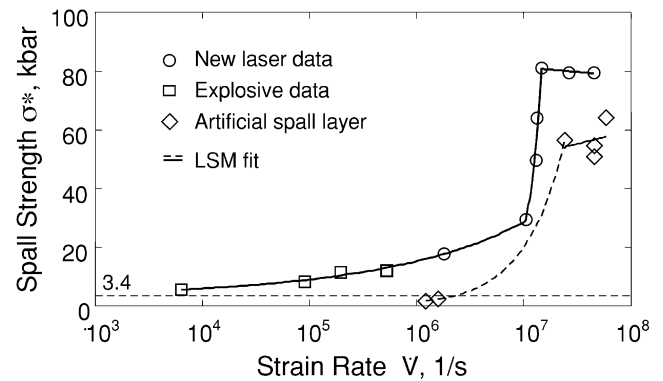


**Fig. 5.** The dependence of the spall strength of an AMg6M aluminum alloy versus strain rate in the dynamic regime of spallation. The explosive data were taken from Bushman *et al.* (1993). The static ultimate strength is 3.4 kbar. The LSM fit is obtained with the method of least squares.

## 5. RESULTS

### 5.1. Dynamic regime of spallation

In the dynamic regime, spallation appears before the negative pressure pulse has reached its maximum, as shown in Figure 4a. The values of the laser spall strength  $\sigma^*$  are shown in Figure 5. Explosive experimental measurements (Bushman *et al.*, 1993) for the same alloy are also shown in this figure. Dynamic spall strength  $\sigma^*$  increases monotonically up to values of strain rate  $\dot{V} \approx 10^7 \text{ s}^{-1}$ :

$$\sigma^* (\text{kbar}) = 0.74 (\dot{V})^{2/9},$$

where the strain rate  $\dot{V}$  is measured in  $\text{s}^{-1}$ . Then the spall strength increases sharply up to a value  $\approx 80$  kbar. This value is the ultimate strength of the AMg6M aluminum alloy. The experiments done with artificial spall layers (lower curve) show that hardening of the material occurs in the plane of contact between the artificial spall layer and the target surface. Indeed in this case the artificial layer is glued to the main target and, initially, in the plane of contact, the strength of material is less than static strength (3.4 kbar). The experimental data for artificial targets show that dynamic strength is greater than static value (except the two first points on the curve in Fig. 5). We conclude therefore that this shows that there is material hardening.

### 5.2. Quasi-stationary regime of spallation

In this case, spallation occurs after the negative pressure pulse has reached its maximum. The material is then in an elongated state during the time  $\Delta t = t_{sp} - t_1$ , where  $t_1$  corresponds to the beginning of the negative pressure pulse (Fig. 4b). Results of experiments in which the negative pressure pulse has a quasi-stationary behavior are shown in Figure 6. In this case, the spall strength  $\sigma^*$  decreases when the duration of the negative pressure pulse  $\Delta t$  is increased:

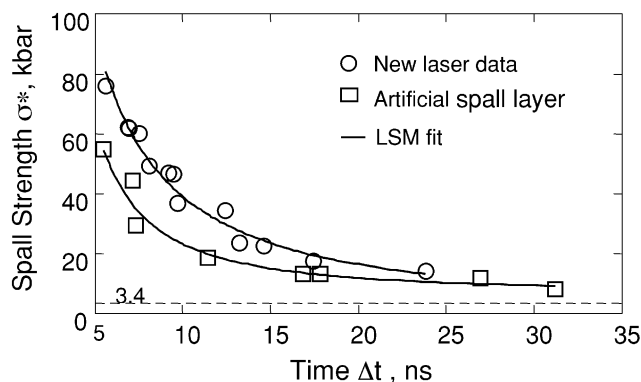


**Fig. 6.** The dependence of the spall strength of an AMg6M aluminum alloy versus the duration of the elongating stress in the quasi-stationary regime. The static ultimate strength is 3.4 kbar; this is known from static measurements in which the load on a sample bar increases slowly (Grigorev & Meilichov, 1991).

$$\sigma^* (\text{kbar}) = 7 \times 10^2 (\Delta t)^{-5/4}$$

where  $\Delta t$  is measured in nanoseconds.

Experiments done with artificial spall layers (lower curve) confirm that also in the quasi-stationary case we have hardening of the material in the plane of contact between the artificial spall layer and the target.

## 6. CONCLUSIONS

1. It was found that two regimes of spallation can exist: dynamic and quasi-stationary.
2. The ultimate dynamic strength of the investigated AMg6M aluminum alloy was measured for the first time.
3. Experiments with artificial spall layers have shown that hardening of material induced by shock-wave compression takes place.

## ACKNOWLEDGMENT

This work was done with the financial support of the Russian Foundation for Basic Research, Grants 00-02-17873 and 00-02-17060.

## REFERENCES

- BATANI D., BENUZZI A., KOENIG M., KRASYUK I., PASHININ P., SEMENOV A., LOMONOSOV I. & FORTOV V. (1999a). Problems of measurement of dense plasma heating in laser shock wave compression *Plasma Phys. Controlled Fusion* **41**, 93–103.
- BATANI D., KOENIG, M., BENUZZI, A., KRASYUK, I.K., PASHININ, P.P., SEMENOV, A.YU., LOMONOSOV, I.V. & FORTOV, V. (1999b). Problems in the optical measurement of dense plasma heating in laser shock-wave compression. *Laser Part. Beams* **17**, 265–273.
- BUSHMAN, A.V., KANEL, G.I., NI, A.L. & FORTOV, V.E. (1993). *Intense Dynamic Loading of Condensed Matter*. London: Taylor and Francis.
- DAHMANI, F. (1993). Experimental scaling laws for mass-ablation rate, ablation pressure in planar laser-produced plasmas with laser intensity, laser wavelength, and target atomic number. *J. Appl. Phys.* **74**, 622–634.
- GRIGOREV, I.S. & MEILICHOV, E.Z., Eds. (1991). *Physical values. Handbook*, p. 53. Moscow–Energoatomizdat.
- IVANOV, V.D. & PETROV, I.B. (1992). Numerical simulation of deformation and fracture under laser interaction with targets. In *Investigation of Physical Processes in Planar and Conical Targets*, Trudy IOFAN [Proc. Gen. Phys. Inst. Russian Acad. Sci.] Vol. 36, pp. 247–266, Moscow: Nauka (in Russian).
- SEMENOV, A.YU. (1997). A modified Courant–Isaacson–Rees method for gas dynamics with an arbitrary equation of state. *Comput. Maths Math. Phys.* **37**, 1334–1340.
- VOVCHENKO, V.I., KRASYUK, I.K., PASHININ, P.P. & SEMENOV, A.YU. (1994). Wide-range dependence of ablation pressure on laser radiation intensity. *J. Russian Acad. Sci. Physics–Doklady* **39**, 633–634.
- ZEL'DOVICH, YA.B. & RAIZER, YU.P. (1967). *Physics of Shock Waves and High-Temperature Hydrodynamic Phenomena*. Vol. 1–2, New York: Academic Press.